

Searching for vector-like leptons decaying into an electron and missing transverse energy in e^+e^- collisions with $\sqrt{s} = 240$ GeV at the FCC-ee

S. Elgammal*

*Centre for Theoretical Physics, The British University in Egypt,
P.O. Box 43, El Sherouk City, Cairo 11837, Egypt.*

(Dated: April 7, 2026)

This analysis delves into the lepton portal dark matter by utilizing Monte Carlo simulated samples from electron-positron collisions at the Future Circular Collider (FCC-ee), operating at a center of mass energy of 240 GeV and an integrated luminosity of 10.8 ab^{-1} . The study explores a specific benchmark scenario in which dark matter is represented as a scalar particle produced as a byproduct of a vector-like lepton. The key signal signature features missing transverse energy alongside dilepton events. Should new physics not be detected, this study establishes 95% confidence level exclusion limits on the mass of the vector-like leptons and the Yukawa coupling.

I. INTRODUCTION

Dark matter is a type of non-visible matter that permeates our universe and is one of the most significant phenomena in physics. Recent astrophysical observations [1, 2] suggested that dark matter makes up about 25% of the universe's energy, while visible matter accounts for only 5%. Evidence for the existence of dark matter has been gathered through various indirect detection methods, such as galaxy rotation curves, gravitational lensing, and the Bullet Cluster [3, 4]. Since these pieces of evidence are based on gravitational effects, the exact nature of dark matter as a particle remains unknown. One promising approach to studying dark matter is through the direct detection of dark matter particles, which are believed to be produced by collisions of high-energy particles in particle accelerators [5, 6].

The Standard Model (SM) of particle physics stands as the most successful framework in the field; however, it does not account for dark matter. This gap highlights the necessity for models beyond the Standard Model (BSMs) that can explain the nature of dark matter particles and their interactions. A viable dark matter candidate must be capable of reproducing the observed relic density of dark matter in the universe. Weakly interacting massive particles (WIMPs) fit this bill well, as they have effectively provided an explanation for the observed relic density of dark matter, a phenomenon often referred to as the WIMP miracle [7].

The lepton portal dark matter model introduced in [8, 9] features a singlet dark matter particle that interacts with the SM gauge group. In this framework, dark matter particles can annihilate into SM leptons via t-channel exchanges of vector-like leptons (VLLs). These VLLs have components that transform identically under the electroweak (EW) gauge group of the SM, which is an intriguing aspect of the model.

Vector-like leptons are a common feature in various BSM theories, including supersymmetry [10–13], grand

unification theories [14–16], and extra-dimensional models [17, 18]. They also play a significant role in dark matter models [19–22]. Additionally, VLLs can account for the mass hierarchy observed among different particle generations [23–25] and may help resolve the gap between the experimentally measured and theoretically predicted values of the anomalous magnetic moment of the muon [12, 26–31].

Searches for singlet and doublet vector-like tau leptons have been conducted by the CMS in both leptonic and hadronic final states [32–34]. These studies have placed constraints on the mass of the doublet vector-like tau leptons, which lie within the range of 120 to 790 GeV. Additionally, the ATLAS experiment has examined vector-like leptons in events featuring hadronic final states, as detailed in [35]. Using Run-2 data, the leptonic channels at ATLAS have been utilized to reinterpret the limits on vector-like leptons decaying into SM leptons of the second generation, as shown in [36].

The analysis presented in reference [37] rules out regions of parameter space where the mass difference between vector-like leptons and dark matter (ΔM) exceeds approximately 100 GeV. More closely related scenarios could be excluded through dedicated searches that take advantage of initial state radiation and soft leptons. However, it is important to note that these limits apply only to a narrow range of parameters, particularly where the mass difference is around 10 GeV, with the most stringent limit being about 250 GeV in the case of a degenerate four-sleptons scenario [30].

In the current study, we will examine the vector-like lepton that decays into a final state consisting of SM electrons and missing transverse energy. Our investigation focuses on two specific scenarios involving the mass difference between the vector-like lepton and the scalar dark matter $\Delta M = 5$ and 10 GeV. The details regarding the production of the vector-like lepton are thoroughly discussed in section II. Since the dark matter particle does not interact with the detector materials, it results in a contribution to the missing transverse energy, denoted as E_T^{miss} . This energy is determined by calculating the vector sum of the transverse energy from visible particles.

* sherif.elgammal@bue.edu.eg

By analyzing this, we aim to identify lepton portal dark matter through the distinctive signature of two electrons coupled with missing transverse energy.

We propose conducting a study on the pair production of vector-like leptons resulting from electron-positron collisions at the Future Circular Collider (FCC-ee) [38] to explore the nature of dark matter. The FCC-ee, an electron-positron collider put forth by CERN, is designed to operate at energy levels between 240 GeV and 365 GeV. While other future lepton colliders, like CLIC [39], are also being considered, our primary focus will remain on the FCC-ee for this research.

The initial phase of the FCC-ee is designed to be a high-luminosity and high-precision electron-positron collider, functioning as a factory for electroweak processes, top quarks, and particularly, the Higgs boson [40]. It provides controllable energy levels and minimizes QCD background noise, making it a crucial tool in this research area.

This paper is organized as follows: In Section II, we provide a brief overview of the theoretical framework for the vector-like lepton portal model. Section III discusses the simulation techniques used to generate both signal and SM background samples. In Section IV, we outline our selection criteria and analysis strategy. Finally, Sections V and VI present a comprehensive overview of our results and a summary of the analysis.

II. THE SIMPLIFIED VLL MODEL

We will examine the lepton portal dark matter model, where the dark matter particle (χ) is a singlet under the SM's gauge group. This dark matter can either be a scalar or a fermion; for our analysis, we will focus on the scalar dark matter case. In this scenario, the mediator is a vector-like lepton. The complete details of this model can be found in [30]. Since χ is a SM singlet, it interacts with the SM via Yukawa couplings (λ_L^i) involving additional leptons that possess the gauge quantum numbers of $(2, -1/2)$ under the electroweak gauge group $SU(2) \times U(1)$.

To prevent anomalies, the extra leptons have been designed to be vector-like. We refer to the electroweak doublet vector-like leptons as L . Additionally, a Z_2 or global $U(1)$ symmetry has been imposed to ensure the stability of dark matter. Under this extra symmetry, all SM fields transform trivially, while the dark matter and the extra leptons undergo non-trivial transformations.

The Lagrangian of the vector-like masses and Yukawa interactions is given by

$$-\mathcal{L} = M_L \bar{L}_L L_R + \lambda_L^i X \bar{L}_i L_R. \quad (1)$$

Vector-like leptons are assumed to couple exclusively to either the first or second generation of the SM leptons. This restriction is implemented to avoid lepton flavor violations, which are strongly constrained by experimental

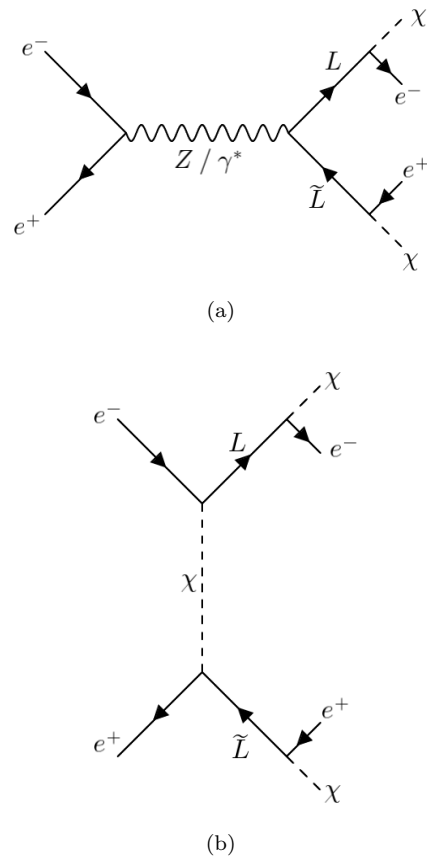


Figure 1 Feynman diagrams of the vector-like lepton pair production for 1(a) s-channel and 1(b) t-channel processes, followed by the decay to the dark matter.

results. In this analysis, we focus on the doublet vector-like lepton that couples to the electron. There are two key parameters relevant to this study: the vector-like lepton mass M_L and the portal Yukawa coupling $\lambda_L := \lambda_L^1$. Here, M_L refers to the mass of the charged component in the doublet, which is crucial for the dilepton plus missing transverse energy (E_T^{miss}) signal examined in this work.

The presence of a light doublet vector-like lepton can potentially increase the mass of the W boson, as suggested by research [31, 45]. This increased mass was reported to be higher than the SM prediction by the CDF collaboration [46]. However, it is important to note that the CDF result has not been confirmed by the CMS and ATLAS collaborations [47, 48].

In this study, we will investigate the production of pairs of vector-like leptons, denoted as L , and their subsequent decay into a SM charged electron and a scalar dark matter particle. The vector-like leptons can be generated through an s-channel process, as illustrated in the Feynman diagram in figure 1(a), where the mediation occurs via Z/γ^* . Alternatively, they can also arise from a t-channel process, depicted in the Feynman diagram in figure 1(b), mediated by the scalar dark matter particle χ . The contribution from the t-channel process is

influenced by the strength of the coupling constant λ_L ; for small values of λ_L , this contribution becomes negligible. The typical signature of this process features two electrons along with significant missing transverse energy, resulting from the stable dark matter particles.

The free parameters in the model are the dark matter mass (M_χ), the vector-like lepton mass (M_L), and the Yukawa coupling (λ_L). The mass-splitting scenario between the vector-like leptons and the dark matter is defined as ΔM .

III. SIMULATION OF SM BACKGROUNDS AND SIGNAL SAMPLES

The SM background processes yielding electron pairs in the signal region are $Z \rightarrow e^+e^-$, and $\rightarrow \tau^+\tau^-$ production, the production of top quark pairs ($t\bar{t} \rightarrow e^+e^- + 2b + 2\nu$), and production of diboson ($W^+W^- \rightarrow e^+e^- + 2\nu$, $ZZ \rightarrow e^+e^- + 2\nu$ and $ZZ \rightarrow 4e$).

The VLL model signal samples and the corresponding SM background samples are privately produced. They have been generated using the WHIZARD event generator 3.1.1 [49, 50]. The ISR effect was included and interfaced with Pythia 6.24 for the parton shower model and hadronization [51]. For a fast detector simulation of the IDEA detector model [52], the DELPHES package [53] was used. These were generated from electron-positron collisions at the FCC-ee with a 240 GeV center of mass energy, which corresponds to the circumstances of RUN I.

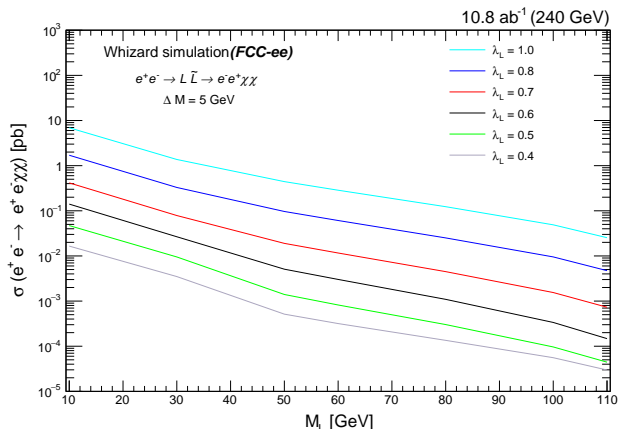


Figure 2 Dependence of cross sections for the signal process $e^+e^- \rightarrow L\tilde{L} \rightarrow e^+e^-\chi\chi$, induced by the VLL model, on the VLL mass with $\sqrt{s} = 240$ GeV for different values of λ_L and $\Delta M = 5$ GeV.

We have generated signal events by creating pairs of vector-like leptons that subsequently decayed into dark matter and SM-charged electrons. This decay process adhered to the following formula:

$$e^+e^- \rightarrow L\tilde{L}, \quad L \rightarrow e^-\chi, \quad \tilde{L} \rightarrow e^+\chi. \quad (2)$$

The study considered different mass-splitting scenarios between the vector-like leptons and the dark matter $\Delta M = 5$ and 10 GeV.

The production of vector-like leptons has been studied via t-channel processes mediated by dark matter, in addition to s-channel production. The decay of the vector-like lepton (L) into an electron and the dark matter particle (χ) has a branching ratio of one. However, the mass of χ significantly impacts the contribution from the t-channel process. If the Yukawa couplings are sufficiently large, the mass of dark matter has a substantial influence on the cross-section.

We conducted several sets of event generation, starting with a small Yukawa coupling of $\lambda_L = 0.4$ and moving up to a larger value of $\lambda_L = 1$. In the case of the small Yukawa coupling, the contribution from the t-channel process is minimal. However, when we examined the larger Yukawa coupling, we observed a significant contribution arising from the t-channel process.

The production cross-sections have been plotted for various λ_L against the mass of the vector-like lepton in figure 2, with a small ΔM scenario ($\Delta M = 5$ GeV). We observe that the production cross section in the scenario with a large Yukawa coupling is significantly larger than in the case with a small Yukawa coupling, indicating that the t-channel process predominates in the former.

The Monte Carlo simulations played a crucial role in generating the SM background samples and calculating their associated cross-sections for this analysis, with the calculations performed at leading order as detailed in Table I. Given the extremely low cross-section value of the leptonic decay of $t\bar{t}$, this process has been excluded from the analysis.

Using these simulations, we estimated the signal samples and the SM background processes, normalizing them to their respective cross sections and an integrated luminosity of 10.8 ab^{-1} .

An ad-hoc flat 10% uncertainty is applied to cover all possible systematic effects.

IV. EVENT SELECTION AND BACKGROUNDS REDUCTION

A. Event pre-selection

The event selection process has been designed to reconstruct a final state consisting of two electrons with low transverse momentum (p_T^e) and missing transverse energy accounting for the invisible particles. The selection is made by applying cuts on various kinematic parameters.

Both electrons must pass a preliminary selection that includes the following criteria:

- p_T^e (GeV) > 5,
- $|\eta^e|$ (rad) < 2.5,
- $E_{had}/E_{em} < 0.1$.

Table I The simulated SM backgrounds generated from electron-positron collisions at the FCC-ee at $\sqrt{s} = 240$ GeV. Their corresponding cross-section times branching ratios for each process, and the generation order are presented. Names of these MC samples and the used generators are stated as well.

Process	Decay channel	Generator	$\sigma \times \text{BR}$ (fb)	Order
Z	e^+e^-	Whizard	2173.0	LO
Z	$\tau^+\tau^-$	Whizard	2231.2	LO
WW	$e^+e^- + 2\nu$	Whizard	202.1	LO
ZZ	$e^+e^- + 2\nu$	Whizard	5.0	LO
ZZ	$4e$	Whizard	0.6	LO
t \bar{t}	$e^+e^- + 2\nu + 2b$	Whizard	1.7×10^{-6}	LO

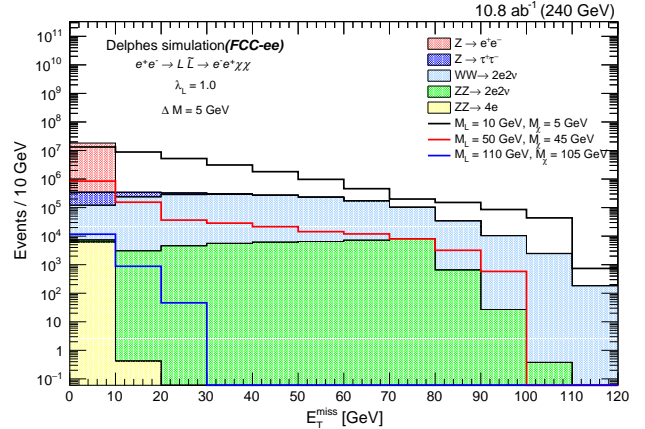
Here, $E_{had}/E_{em} < 0.1$ represents the criterion that examines the ratio of energy deposited in the hadronic calorimeter (E_{had}) to that in the electromagnetic calorimeter (E_{em}). This ratio should be less than 10%. These pre-selection cuts are listed in Table II. Each event is selected based on two opposite-charge electrons.

Table II Summary of cut-based event selections used in the analysis.

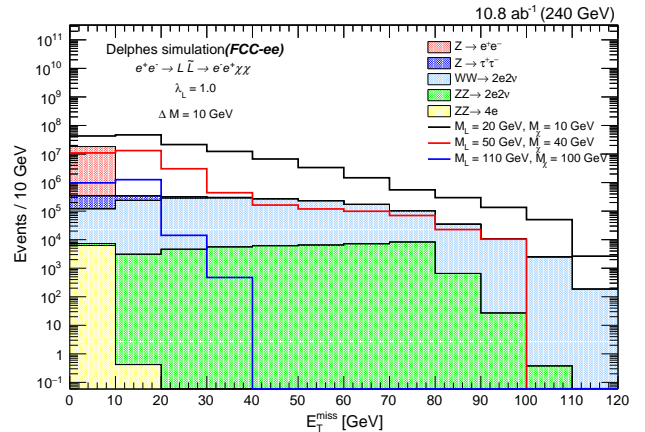
Pre-selection	Final selection
$p_T^e > 5$ GeV	$p_T^e > 5$ GeV
$ \eta^e < 2.5$ rad	$ \eta^e < 2.5$ rad
$E_{had}/E_{em} < 0.1$	$E_{had}/E_{em} < 0.1$
	$ p_T^{e^+e^-} - E_T^{miss} /p_T^{e^+e^-} < 0.1$
	$\Delta R(e^+e^-) < 3.0$
	$\cos(\text{Angle}_{3D}) < -0.9$

Figure 3 illustrates the distribution of the missing transverse energy (E_T^{miss}) for events that passed the pre-selection criteria outlined in table II, with $E_T^{miss} < 120$ GeV. In this visualization, the red histogram represents the $Z \rightarrow e^+e^-$ background, while the blue histogram illustrates $Z \rightarrow \tau\tau$ background. The cyan histogram indicates the vector boson pair background (WW). The green histogram corresponds to the process $ZZ \rightarrow 2e2\nu$, and the yellow histogram depicts the $ZZ \rightarrow 4e$ events. These histograms are presented in a stacked format. While the signals of the VLL model, which have been generated with different masses ($M_L = 10, 50,$ and 110 GeV) and fixing the coupling constants $\lambda_L = 1.0$ and $\Delta M = 5$ GeV in 3(a) and 10 GeV in 3(b), are represented by different colored lines, and are overlaid.

Figure 3 shows that the signal samples are significantly mixed with background events across the entire E_T^{miss} spectrum, particularly for $M_L = 50, 110$ GeV, and $\Delta M = 5$ GeV. Therefore, as discussed in the following paragraph, it is necessary to establish stricter criteria to effectively differentiate the signals from the SM backgrounds.



(a)



(b)

Figure 3 The measured missing transverse energy (E_T^{miss}) spectrum, after applying pre-selection summarized in table II, for the estimated SM backgrounds and different choices of VLL masses generated based on the VLL model, with $\lambda_L = 1.0$ and $\Delta M = 5$ GeV in 3(a), and 10 GeV in 3(b).

B. Event final selection and efficiencies

In addition to the pre-selection criteria, we have applied tighter cuts based on four variables:

1. We assess the relative difference between the trans-

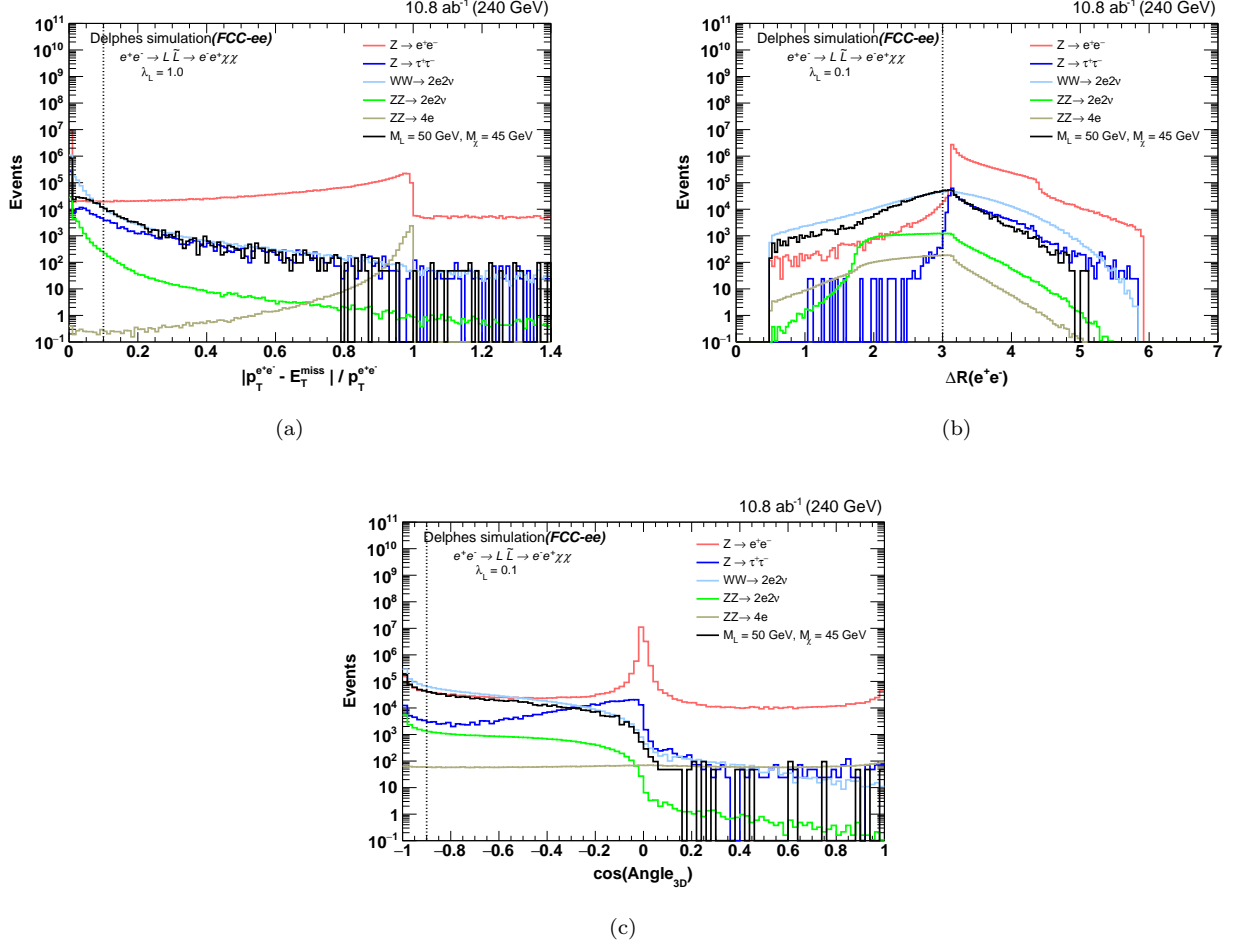


Figure 4 The distributions of three variables for dielectron events, where each electron passes the low p_T electron ID discussed in the pre-selection in table II. The four variables are $|p_T^{e^+e^-} - E_T^{miss}|/p_T^{e^+e^-}$ 4(a), $\Delta R(e^+e^-)$ 4(b), and $\cos(\text{Angle}_{3D})$ 4(c). The model corresponds to the VLL with different values of $M_L = 50$ GeV and $M_\chi = 45$ GeV, and for the SM backgrounds. The vertical dashed lines correspond to the chosen cut value for each variable.

verse momentum of the dielectron ($p_T^{e^+e^-}$) and the missing transverse energy (E_T^{miss}). This difference is selected to be less than 0.1, defined by the condition $|p_T^{e^+e^-} - E_T^{miss}|/p_T^{e^+e^-} < 0.1$.

2. We impose a cut on the angular separation $\Delta R(e^+e^-)$ between the two opposite-sign electrons, which must be less than 3.0.

3. We apply a criterion on the cosine of the 3D angle between the missing energy vector and the dielectron system vector to ensure they are back-to-back, requiring that $\cos(\text{Angle}_{3D}) < -0.9$.

The plots in Figure 4 illustrate the distributions of specific variables for a single signal presentation of the VLL model, with an M_L value of 50 GeV and a dark matter mass ($M_\chi = 45$ GeV). Additionally, the figures include the SM backgrounds. These variables are presented for both the VLL signal sample and the SM backgrounds in relation to dielectron events that meet the pre-selection

criteria outlined in Table II.

The first variable is represented as $|p_T^{e^+e^-} - E_T^{miss}|/p_T^{e^+e^-}$, with its graph displayed in Figure 4(a). The second variable measures the variable, the angular distance between the two electrons, referred to as $\Delta R(e^+e^-)$, is presented in Figure 4(b). Lastly, $\cos(\text{Angle}_{3D})$, is illustrated in Figure 4(c). The vertical dashed lines in these figures indicate the selected cut value for each variable.

The performance metrics for fine-tuning these rigorous cuts are illustrated by plotting the N-1 efficiency for each of the four criteria detailed in Table II. To calculate the N-1 efficiency, we count the number of events that pass the final selection and divide it by the number that would have cleared it in the absence of the specific cut under consideration.

In figure 5, we present the distributions of the N-1 efficiencies plotted against the transverse momentum

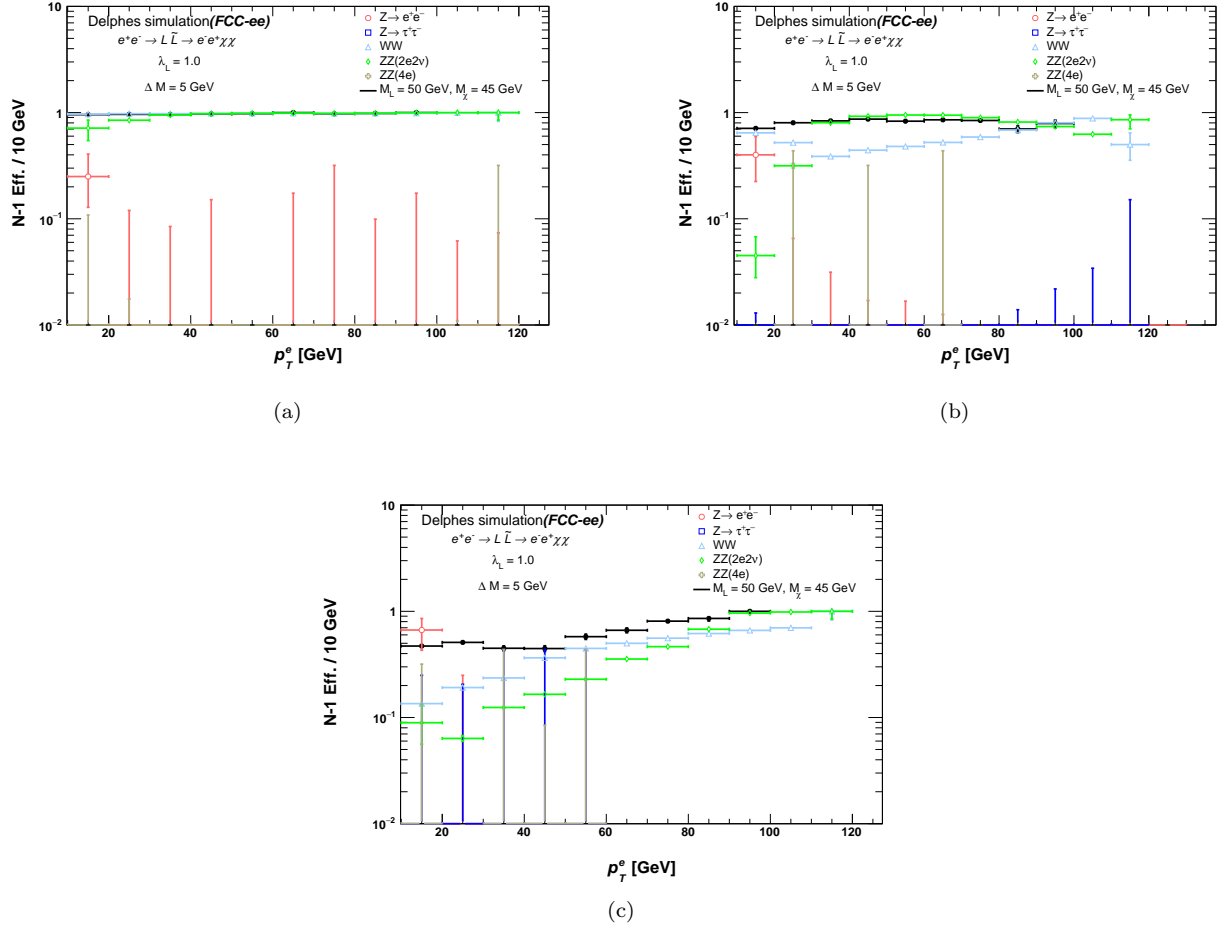


Figure 5 Distributions of the N-1 efficiencies plotted against the transverse momentum of the leading reconstructed electron (p_T^e) for the following cuts; $|p_T^{e^+e^-} - E_T^{miss}|/p_T^{e^+e^-} < 0.1$ 5(a), $\Delta R(e^+e^-) < 3.0$ 5(b), and $\cos(\text{Angle}_{3D}) < -0.9$ 5(c) for the signal in the VLL model with $\Delta M = 5$ GeV and for the SM backgrounds.

of the leading reconstructed electron (p_T^e) for the following conditions: $|p_T^{e^+e^-} - E_T^{miss}|/p_T^{e^+e^-} < 0.1$ 5(a), $\Delta R(e^+e^-) < 3.0$ 5(b), and $\cos(\text{Angle}_{3D}) < -0.9$ 5(c). These Figures focus on the signal in the VLL model (indicated by black closed circles), with $M_L = 50$ GeV, $M_\chi = 45$ and $\lambda_L = 1.0$, alongside SM backgrounds marked with open colored markers.

The cut on the ratio $|p_T^{e^+e^-} - E_T^{miss}|/p_T^{e^+e^-}$ significantly reduces the occurrences of $Z \rightarrow e^+e^-$, $\tau\tau$ and $ZZ(4e)$ events. Additionally, the $\Delta R(e^+e^-)$ cut decreases the contamination of $Z \rightarrow e^+e^-$, $\tau\tau$, $ZZ(4e)$, and WW events. Furthermore, the $\cos(\text{Angle}_{3D})$ cut results in a reduction of $Z \rightarrow e^+e^-$, $\tau\tau$, $ZZ(4e)$, WW, and $ZZ(2e2\nu)$ events.

For the signal, the results show a flat efficiency across all selection criteria with respect to p_T^e , except for the $\cos(\text{Angle}_{3D})$ cut, which demonstrates a decline at low p_T^e (specifically for $p_T^e < 50$ GeV). Nonetheless, the implementation of this cut is crucial for reducing contami-

nation from WW and $ZZ(2e2\nu)$ events.

Ultimately, the application of these three stringent selection criteria significantly suppresses the background from the processes $Z \rightarrow \tau\tau$ and $ZZ(4e)$. This strategy also minimizes contamination from other events, including WW, $ZZ(2e2\nu)$, and $Z \rightarrow e^+e^-$.

V. RESULTS

The study's results were drawn using a shape-based analysis, where the variable E_T^{miss} serves as the key differentiator. Figure 6 illustrates the distributions of missing transverse energy for both SM backgrounds and the signal samples, considering vector-like lepton with $\Delta M = 5$ GeV in 6(a) and 10 GeV in 6(b). These distributions pertain to the electro-philic scenario with $\lambda_L = 1.0$, generated from electron-positron collisions at the FCC-ee. The collisions occur at a center-of-mass energy of $\sqrt{s} = 240$ GeV, with an integrated luminosity of 10.8 ab^{-1} . The

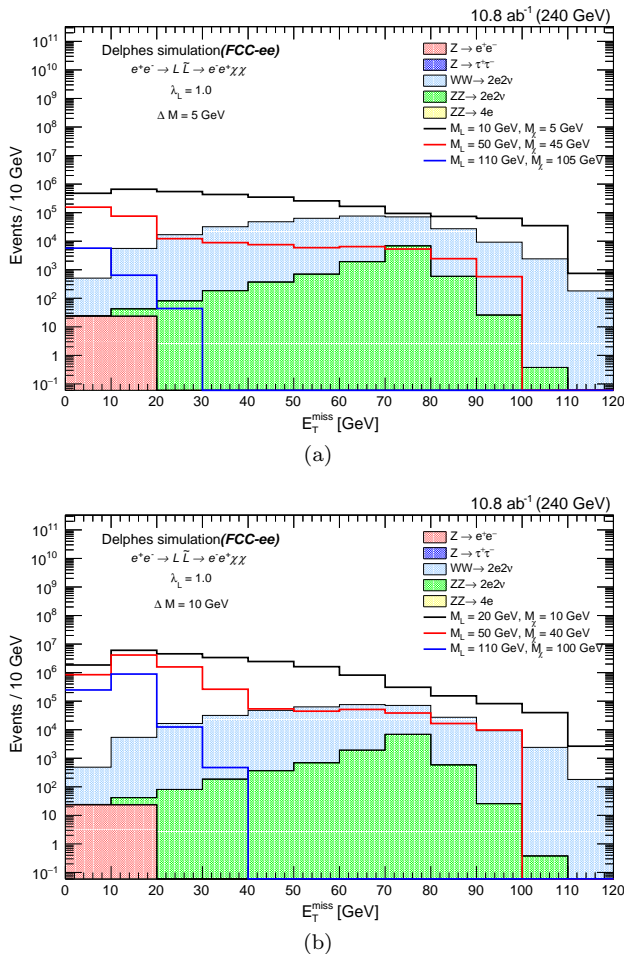


Figure 6 The spectrum of missing transverse momentum (E_T^{miss}), for events passing the final selection listed in table II, for the estimated SM backgrounds and different choices of the VLL masses generated based on the VLL model, with the coupling constants $\lambda_L = 1.0$ and $\Delta M = 5$ GeV in 6(a) and 10 GeV in 6(b).

event selection is based on the final cuts summarized in Table II.

Table III outlines the number of events that successfully met both the pre-selection criteria (shown in the middle column) and the full selection criteria (indicated in the right column). These results were derived from simulations that accounted for both backgrounds and three VLL signal samples, as detailed in the first column. The simulations were performed with a luminosity of 10.8 ab^{-1} at $\sqrt{s} = 240$ GeV. The signal sample is based on the VLL model, with model parameters set to $\Delta M = 5.0$ GeV, and $\lambda_L = 1.0$. We incorporated total uncertainties that cover both statistical and systematic components for the simulated signal and background samples.

We used the profile likelihood method to analyze our results statistically and performed a statistical test based on the E_T^{miss} distributions. We used the modified frequentist construction CLs [56, 57], which is based on the

asymptotic approximation [55], to derive exclusion limits on the product of signal cross sections at a 95% confidence level. In the likelihood, the systematic uncertainties are treated as nuisance parameters.

Figure 7 illustrates the 95% confidence level (CL) limits on the cross-section for the vector-like lepton simplified model, focusing on the electronic decay of L . The results are based on a narrow mass splitting of $\Delta M = 5$ GeV 7(a), and 10 GeV 7(b) derived from an integrated luminosity of 10.8 ab^{-1} at a center-of-mass energy of $\sqrt{s} = 240$ GeV. The limits are represented by distinct colored solid lines, each corresponding to different values of the coupling constant λ_L . Additionally, the statistical test provides an expected limit shown as a dashed line, while the green and yellow bands indicate the ± 1 and ± 2 sigma ranges, respectively.

The results for the VLL model are also interpreted in the $M_L - \lambda_L$ plane for two different ΔM values: 5, 10 GeV. Since the shape of the E_T^{miss} distribution almost does not change with λ_L , and affects only the product of the VLL production cross section, the limit shown in figure 7 can be simply rescaled for different values of λ_L , from 0.6 to 1.0 for $\Delta M = 5$ GeV, and from 0.43 to 1.0 for $\Delta M = 10$ GeV. These limits, in the $M_L - \lambda_L$ plane, are shown in Figure 8. The shaded areas enclosed by the contour for given values of $\Delta M = 5$ and 10 GeV are excluded at 95% CL.

The expected limits indicate that the mass of the vector-like lepton (VLL) can be excluded in the range of 10 to 74.6 GeV when the coupling constant $\lambda_L = 1.0$, with a mass difference (ΔM) of 5 GeV and an integrated luminosity of 10.8 ab^{-1} at a center-of-mass energy of $\sqrt{s} = 240$ GeV. For a mass difference of 10 GeV, M_L is excluded in the range from 20 to 110 GeV when λ_L varies between 0.75 and 1.0.

The FCC-ee may not have sufficient sensitivity to investigate the VLL model, especially in scenarios where λ_L is below 0.6 with a narrow mass splitting of $\Delta M = 5$ GeV. Additionally, it lacks sensitivity for λ_L values below 0.43 when $\Delta M = 10$ GeV.

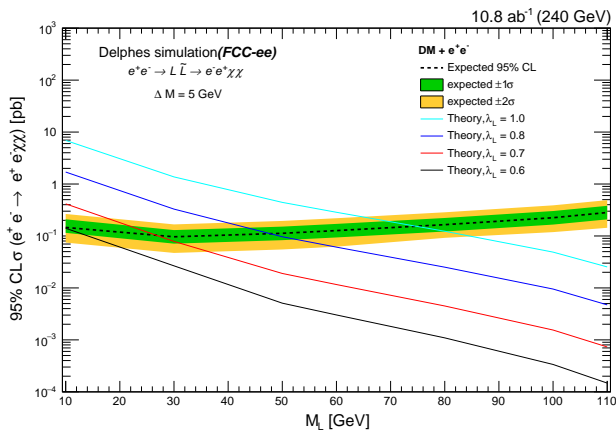
VI. SUMMARY

The Future Circular Collider (FCC-ee) is a proposed lepton collider that would collide beams of electrons and positrons. The FCC-ee will be capable of scanning the center-of-mass energies from 240 to 365 GeV. One of the main aims of the FCC-ee is to discover physics beyond the SM.

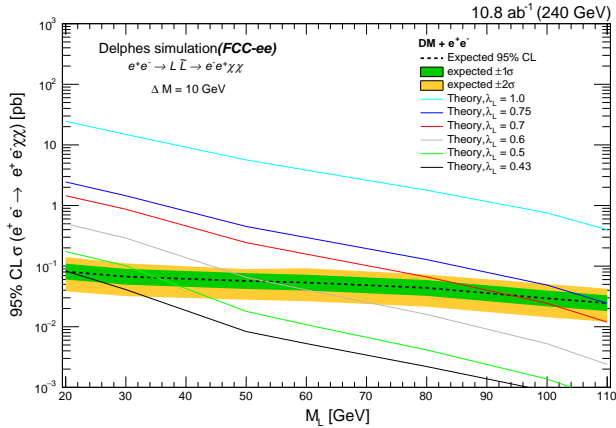
In our analysis, we investigated the possibility of producing the lepton portal dark matter. We focused on the electron-philic scalar dark matter scenario, where the dark matter is created from the decay of extra vector-like leptons, which are produced in pairs from electron-positron collisions at the FCC-ee with a center-of-mass energy of 240 GeV. These vector-like leptons can decay into a scalar dark matter and an electron. We have

Table III The Table summarizes the number of events that met the pre-selection (middle column) and full selection (right column) criteria from simulations for SM backgrounds and a signal, conducted with a luminosity of 10.8 ab^{-1} at $\sqrt{s} = 240 \text{ GeV}$. The signal corresponds to the VLL model with $\Delta M = 5 \text{ GeV}$, $\lambda_L = 1.0$. The total uncertainties, which include both statistical and systematic components, have been combined using the quadratic form. Signal significance against the SM background is shown before and after the final selection.

Process	No. of events passing pre-selection	No. of events passing final-selection
$Z \rightarrow e^+e^-$	17914760.6 ± 1791481.1	46.9 ± 8.3
$Z \rightarrow \tau^+\tau^-$	392856.0 ± 39290.6	0 ± 0
$WW \rightarrow e^+e^- + 2\nu$	1697677.2 ± 169772.7	342080.9 ± 34213.1
$ZZ \rightarrow e^+e^- + 2\nu$	43063.7 ± 4311.4	10763.3 ± 1081.3
$ZZ \rightarrow 4e$	6254.1 ± 630.4	0.0 ± 0.0
Sum Bkgs	20054611.6 ± 2005466.2	352891.1 ± 35294.1
Signal of VLL model (at $M_L = 10 \text{ GeV}$ and $M_\chi = 5 \text{ GeV}$) (at $M_L = 50 \text{ GeV}$ and $M_\chi = 45 \text{ GeV}$) (at $M_L = 110 \text{ GeV}$ and $M_\chi = 105 \text{ GeV}$)	34222019.0 ± 3422206.9 1126939.4 ± 112698.9 12618.9 ± 1266.9	3161226.7 ± 316127.7 280667.8 ± 28071.7 6394.6 ± 644.4



(a)



(b)

Figure 7 95% C.L. limit on the expected production cross-section of the vector-like leptons as a function of the vector-like lepton mass. The solid colored lines represent the cross-section predicted from the electro-philic vector-like lepton theory with several values of Yukawa coupling (λ_L) and $\Delta M = 5 \text{ GeV}$ 7(a), and 10 GeV 7(b).

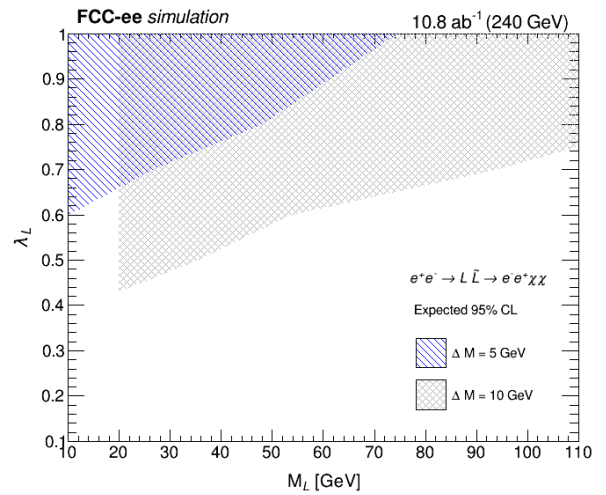


Figure 8 The upper limits at 95% CL on the expected cross section for the VLL model in the M_L and λ_L plane at $\sqrt{s} = 240 \text{ GeV}$. Each contour represents the excluded region for a given value of $\Delta M = 5$, and 10 GeV .

simulated signal and background samples produced from electron-positron collisions at a center-of-mass energy of 240 GeV , and 10.8 ab^{-1} of integrated luminosity corresponds to FCC-ee Run I.

This analysis, based on the events that passed the final selection, allowed us to set upper limits on the production cross-section. Additionally, we established an exclusion limit for the mass of the doublet vector-like lepton L . This was done under a certain scenario for the mass splitting between the vector-like lepton and the dark matter, specifically with narrow ΔM values of 5 and 10 GeV , while varying the Yukawa coupling (λ_L).

In this scenario, with a narrow mass splitting of $\Delta M = 5 \text{ GeV}$, we have ruled out vector-like lepton masses up to 74.6 GeV when the coupling constant $\lambda_L = 1.0$. This analysis is based on an integrated luminosity of 10.8 ab^{-1}

at a center-of-mass energy of $\sqrt{s} = 240$ GeV. However, for values of λ_L below 0.6, the FCC-ee will not have the sensitivity necessary to probe the vector-like lepton model. For $\Delta M = 10$ GeV, wider ranges of M_L and λ_L can be excluded.

This study highlights the potential to explore scenarios where vector-like leptons are nearly degenerate with dark matter, specifically when $\Delta M \ll 100$ GeV—an area that the LHC could not reach.

The findings pertaining to the muon-philic scenario would closely mirror those detailed in this study, provided that the reconstruction efficiencies and resolutions for electrons and muons are on par. In contrast, the sensitivities for the tau-philic scenario are anticipated to be less robust due to the intricate nature of tau signals

within the detector. However, in-depth investigations into these particular cases fall outside the scope of this paper.

ACKNOWLEDGMENTS

The author of this paper wishes to express gratitude to J. Kawamura, co-author of [30], for supplying the UFO model files, assisting with the generation of signal events, and validating the results through cross-checking. In addition, this paper is based on works supported by the Science, Technology, and Innovation Funding Authority (STDF) under grant number 48289.

-
- [1] Planck Collaboration, Planck 2015 results. XIII. Cosmological parameters, *Astron. Astrophys.* 594 (2016) A13 [[arXiv:1502.01589](#)] [[iNSPIRE-HEP](#)].
- [2] *Planck 2018 results. VI. Cosmological parameters.* A&A 641, A6 (2020) [[arXiv:1807.06209](#)] [[astro-ph.CO](#)].
- [3] Lage, C and Farrar, G, The bullet cluster is not a cosmological anomaly, *JCAP*, vol. 2015, no. 2, 038. [[https://doi.org/10.1088/1475-7516/2015/02/038](#)].
- [4] Bertone, Gianfranco and Hooper, Dan and Si, Particle dark matter: Evidence, candidates and constraints, *Phys. Rept.* 405 (2005) 279-390 [[arXiv:hep-ph/0404175](#)] [[iNSPIRE-HEP](#)].
- [5] CMS Collaboration, Dark sector searches with the CMS experiment - 2024, DOI: [https://arxiv.org/abs/2405.13778](#)
- [6] Haley Joseph, Searches for Dark Matter with the ATLAS Experiment at the LHC, 2023, [https://cds.cern.ch/record/2846383](#)
- [7] Scherrer, Robert J. and Turner, Michael S., On the relic, cosmic abundance of stable, weakly interacting massive particles, *Phys. Rev. D* 33 (1986) 1585 [[iNSPIRE-HEP](#)].
- [8] S. Chang, R. Edezhath, J. Hutchinson and M. Luty, “Leptophilic Effective WIMPs,” *Phys. Rev. D* **90** (2014) no.1, 015011 [[arXiv:1402.7358](#)] [[hep-ph](#)].
- [9] Y. Bai and J. Berger, “Lepton Portal Dark Matter,” *JHEP* **08** (2014), 153 doi:10.1007/JHEP08(2014)153 [[arXiv:1402.6696](#)] [[hep-ph](#)].
- [10] S. P. Martin, “Extra vectorlike matter and the lightest Higgs scalar boson mass in low-energy supersymmetry”, *Phys. Rev. D* 81 (2010) 035004, doi:10.1103/PhysRevD.81.035004, [[arXiv:0910.2732](#)].
- [11] S. Zheng, “Minimal vectorlike model in supersymmetric unification”, *Eur. Phys. J. C* 80 (2020) 273, doi:10.1140/epjc/s10052-020-7843-8, [[arXiv:1904.1014](#)]
- [12] M. Endo, K. Hamaguchi, S. Iwamoto, and N. Yokozaki, “Higgs mass and muon anomalous magnetic moment in supersymmetric models with vectorlike matters”, *Phys. Rev. D* 84 (2011) 075017, doi:10.1103/PhysRevD.84.075017, [[arXiv:1108.3071](#)].
- [13] K. Kong, S. C. Park, and T. G. Rizzo, “A vector-like fourth generation with a discrete symmetry from Split-UED”, *JHEP* 07 (2010) 059, doi:10.1007/JHEP07(2010)059, [[arXiv:1004.4635](#)].
- [14] R. Nevzorov, “E6 inspired supersymmetric models with exact custodial symmetry”, *Phys. Rev. D* 87 (2013) 015029, doi:10.1103/PhysRevD.87.015029, [[arXiv:1205.5967](#)].
- [15] I. Doršner, S. Fajfer, and I. Mustafic, “Light vector-like fermions in a minimal SU(5) setup”, *Phys. Rev. D* 89 (2014) 115004, doi:10.1103/PhysRevD.89.115004, [[arXiv:1401.6870](#)].
- [16] A. Joglekar and J. L. Rosner, “Searching for signatures of E6”, *Phys. Rev. D* 96 (2017)015026, doi:10.1103/PhysRevD.96.015026, [[arXiv:1607.06900](#)].
- [17] G.-Y. Huang, K. Kong, and S. C. Park, “Bounds on the fermion-bulk masses in models with universal extra dimensions”, *JHEP* 06 (2012) 099, doi:10.1007/JHEP06(2012)099, [[arXiv:1204.0522](#)].
- [18] K. Kong, S. C. Park, and T. G. Rizzo, “A vector-like fourth generation with a discrete symmetry from Split-UED”, *JHEP* 07 (2010) 059, doi:10.1007/JHEP07(2010)059, [[arXiv:1004.4635](#)].
- [19] P. Schwaller, T. M. P. Tait, and R. Vega-Morales, “Dark matter and vectorlike leptons from gauged lepton number”, *Phys. Rev. D* 88 (2013) 035001, doi:10.1103/PhysRevD.88.035001, [[arXiv:1305.1108](#)]
- [20] J. Halverson, N. Orlofsky, and A. Pierce, “Vectorlike leptons as the tip of the dark matter iceberg”, *Phys. Rev. D* 90 (2014) 015002, doi:10.1103/PhysRevD.90.015002, [[arXiv:1403.1592](#)].
- [21] S. Bahrami et al., “Dark matter and collider studies in the left-right symmetric model with vectorlike leptons”, *Phys. Rev. D* 95 (2017) 095024, doi:10.1103/PhysRevD.95.095024, [[arXiv:1612.06334](#)]
- [22] S. Bhattacharya, P. Ghosh, N. Sahoo, and N. Sahu, “Mini review on vector-like leptonic dark matter, neutrino mass, and collider signatures”, *Front. Phys.* 7 (2019) 80, doi:10.3389/fphy.2019.00080, [[arXiv:1812.06505](#)]
- [23] A. Falkowski, D. M. Straub, and A. Vicente, “Vectorlike leptons: Higgs decays and collider phenomenology”, *JHEP* 05 (2014) 092, doi:10.1007/JHEP05(2014)092, [[arXiv:1312.5329](#)].
- [24] K. Agashe, T. Okui, and R. Sundrum, “Common origin for neutrino anarchy and charged hierarchies”, *Phys. Rev. Lett.* 102 (2009) 101801, doi:10.1103/PhysRevLett.102.101801, [[arXiv:0810.1277](#)].

- [25] M. Redi, “Leptons in composite MFV”, JHEP 09 (2013) 060, doi:10.1007/JHEP09(2013)060, arXiv:1306.1525.
- [26] Radovan Dermisek, Aditi Raval, ”Explanation of the muon g-2 anomaly with vectorlike leptons and its implications for Higgs decays”, Phys. Rev. D 88 (2013) 013017, doi:10.1103/PhysRevD.88.013017, arXiv:1305.3522
- [27] Eugenio Megias, Mariano Quiros, and Lindber Salas, ” $g_\mu - 2$ from vector-like leptons in warped space”, JHEP 05 (2017) 016, doi:10.1007/JHEP05(2017)016, arXiv:1701.05072.
- [28] J. Kawamura, S. Raby, and A. Trautner, “Complete vectorlike fourth family and new $U(1)'$ for muon anomalies”, Phys. Rev. D 100 (2019) 055030, doi:10.1103/PhysRevD.100.055030, arXiv:1906.11297
- [29] G. Hiller, C. Hormigos-Feliu, D. F. Litim, and T. Steudtner, “Model building from asymptotic safety with Higgs and flavor portals”, Phys. Rev. D 102 (2020) 095023, doi:10.1103/PhysRevD.102.095023, arXiv:2008.08606.
- [30] Junichiro Kawamura, Shohei Okawa, Yuji Omura, Current status and muon g-2 explanation of lepton portal dark matter, JHEP 08 (2020) 042.
- [31] J. Kawamura, S. Okawa and Y. Omura, “W boson mass and muon g-2 in a lepton portal dark matter model,” Phys. Rev. D **106** (2022) no.1, 015005 doi:10.1103/PhysRevD.106.015005 [arXiv:2204.07022 [hep-ph]].
- [32] CMS Collaboration, “Search for vector-like leptons in multilepton final states in proton-proton collisions at $\sqrt{s} = 13$ TeV”, Phys. Rev. D 100 (2019) 052003, doi:10.1103/PhysRevD.100.052003, arXiv:1905.10853.
- [33] CMS Collaboration, “Inclusive nonresonant multilepton probes of new phenomena at $\sqrt{s} = 13$ TeV”, Phys. Rev. D 105 (2022) 112007, doi:10.1103/PhysRevD.105.112007, arXiv:2202.08676.
- [34] CMS Collaboration, Search for pair-produced vector-like leptons in final states with third-generation leptons and at least three b quark jets in proton-proton collisions at $\sqrt{s} = 13$ TeV, Phys. Lett. B 846 (2023) 137713, doi:10.1016/j.physletb.2023.137713, arXiv:2208.09700.
- [35] ATLAS Collaboration, Search for electroweak production of vector-like leptons in multiple τ -lepton and b -jets final states in pp collisions at $\sqrt{s}=13$ TeV with the ATLAS detector, Eur. Phys. J. C 85 (2025) 1335.
- [36] J. Kawamura and S. Shin, Current status on pair-produced muon-philic vectorlike leptons in multilepton channels at the LHC, JHEP **11** (2023), 025 doi:10.1007/JHEP11(2023)025 [arXiv:2308.07814 [hep-ph]].
- [37] ATLAS collaboration, Search for electroweak production of charginos and sleptons decaying into final states with two leptons and missing transverse momentum in $\sqrt{s}=13$ TeV pp collisions using the ATLAS detector, Eur. Phys. J. C 80 (2020) 123 [arXiv:1908.08215] [INSPIRE].
- [38] I. Agapov et. al., Future Circular Lepton Collider FCC-ee: Overview and Status. DOI: <https://doi.org/10.48550/arXiv.2203.08310>
- [39] M. Aicheler et.al., The Compact Linear Collider (CLIC) - Project Implementation Plan, DOI: <https://e-publishing.cern.ch/index.php/CYRM/issue/view/68>
- [40] S. Alipour-Fard, N. Craig, M. Jiang and S. Koren, Long Live the Higgs Factory: Higgs Decays to Long-Lived Particles at Future Lepton Colliders, Chin. Phys. C 43 (2019) 053101 [1812.05588].
- [41] J. Brau, Y. Okada, N. Walker, arXiv:0712.1950 [physics.acc-ph].
- [42] A. Djouadi et al, arXiv:0709.1893 [hep-ph].
- [43] N. Phinney, N. Toge, N. Walker, arXiv:0712.2361 [physics.acc-ph].
- [44] T. Behnke et al., ArXiv e-prints (2007) arXiv:0712.2356 [physics.ins-det]
- [45] J. Kawamura and S. Raby, “W mass in a model with vectorlike leptons and $U(1)'$,” Phys. Rev. D **106** (2022) no.3, 035009 doi:10.1103/PhysRevD.106.035009 [arXiv:2205.10480 [hep-ph]].
- [46] T. Aaltonen *et al.* [CDF], “High-precision measurement of the W boson mass with the CDF II detector,” Science **376** (2022) no.6589, 170-176 doi:10.1126/science.abk1781
- [47] CMS collaboration, High-precision measurement of the W boson mass with the CMS experiment at the LHC, 2024, arXiv:2412.13872 [hep-ex].
- [48] ATLAS collaboration, Measurement of the W -boson mass and width with the ATLAS detector using proton-proton collisions at $\sqrt{s} = 7$ TeV, Eur. Phys. J. C 84 (2024) 1309
- [49] Wolfgang Kilian, Thorsten Ohl, and Jurgen Reuter. WHIZARD—simulating multi-particle processes at LHC and ILC. The European Physical Journal C, 71(9), Sep 2011.
- [50] T. Ohl. O’Mega & WHIZARD: Monte Carlo event generator generation for future colliders. DOI:10.1063/1.1394396
- [51] T. Sjostrand, S. Mrenna and P. Skands, PYTHIA 6.4 Physics and Manual [arXiv:hep-ph/0603175].
- [52] The IDEA detector concept for FCC-ee (2025). arXiv:2502.21223 [physics.ins-det].
- [53] J. de Favereau, C. Delaere, P. Demin, A. Giammanco, V. Lemaître, A. Mertens, M.Selvaggi, DELPHES 3, A modular framework for fast simulation of a generic collider experiment, JHEP 1402 (2014).
- [54] Ferro, Cristina, B-tagging in CMS, EPJ Web of Conferences 28 12055 (2012), DOI: 10.1051/epj-conf/20122812055.
- [55] G. Cowan et al., Asymptotic formulae for likelihood-based tests of new physics, Eur. Phys. J. C 71 (2011), p. 1554, doi: 10.1140/epjc/s10052-011-1554-0, arXiv:1007.1727 [physics.data-an], Erratum: Eur. Phys. J. C 73 (2013) 2501.
- [56] A. L. Read, Presentation of search results: the CLs technique, J. Phys. G: Nucl. Part.Phys. 28 (2002) 2693, doi:10.1088/0954-3889/28/10/313.
- [57] T. Junk, Confidence level computation for combining searches with small statistics, Nuclear Instruments and Methods in Physics Research Section A: Accelerators, Spectrometers, Detectors and Associated Equipment, Volume 434, Issues 2–3, 1999, Pages 435-443, ISSN 0168-9002, [https://doi.org/10.1016/S0168-9002\(99\)00498-2](https://doi.org/10.1016/S0168-9002(99)00498-2).